

Formation of heavy-meson bound states by two-nucleon pick-up reactions

N. Ikeno,¹ J. Yamagata-Sekihara,^{2,3} H. Nagahiro,¹ D. Jido,³ and S. Hirenzaki¹

¹*Department of Physics, Nara Woman's University, Nara 630-8506, Japan*

²*Departamento de Física Teórica and IFIC, Centro Mixto Universidad de Valencia–CSIC, Institutos de Investigación de Paterna, Aptdo. 22085, ES-46071 Valencia, Spain*

³*Yukawa Institute for Theoretical Physics, Kyoto University, Kyoto 606-8502, Japan*

(Received 8 June 2011; revised manuscript received 27 September 2011; published 9 November 2011)

We develop a model to evaluate the formation rate of the heavy mesic nuclei in two-nucleon pick-up reactions and apply it to the ${}^6\text{Li}$ target cases for the formation of heavy meson- α bound states, as examples. The existence of the quasideuteron in the target nucleus is assumed in this model. It is found that mesic nuclei formation in recoilless kinematics is possible even for heavier mesons than the nucleon in two-nucleon pick-up reactions. We find the formation rate of the meson- α bound states can be around half of the elementary cross sections at the recoilless kinematics with small distortions.

DOI: [10.1103/PhysRevC.84.054609](https://doi.org/10.1103/PhysRevC.84.054609)

PACS number(s): 21.85.+d, 36.10.Gv, 25.10.+s, 13.60.Le

I. INTRODUCTION

Meson-nucleus systems are one of the most interesting laboratories to study the meson properties at finite density and to explore the symmetry breaking pattern of QCD and its partial restoration in the nucleus [1–3]. Studies of especially the bound states of the meson and the nucleus have the following advantages: (i) the selective observation of the meson properties is possible by making use of the fixed quantum numbers of the bound states, (ii) the meson properties inside the nucleus can be observed clearly only with relatively small contamination from the vacuum processes, and (iii) the system is quasistatic and the time-dependent dynamical evolution of the system is irrelevant. These features are different from other methods based on scattering and collision processes. On the other hand, information obtained from the observation of the bound states is limited to the $\rho \lesssim \rho_0$ and $T = 0$ region of the QCD phase diagram.

We have studied so far the physical interests, the structures, and the formation reactions of various kinds of meson-nucleus systems [4–6]. Within these studies, the most exciting and successful results were obtained by the observation of deeply bound pionic atoms in the one-nucleon pick-up ($d, {}^3\text{He}$) reactions [2,4,7]. We have also considered other one-nucleon pick-up reactions such as (γ, p) [8] and (π, N) [9] for mesic nuclei formation. The one-nucleon pick-up reactions are found to be useful for the mesic nucleus formation; however, they require large momentum transfer for heavy-meson production, which is one of the main obstacles to observing bound states. Thus, we need to develop new methods for bound-state formation to extend our studies to other meson-nucleus systems, especially for heavier mesons. We are specifically interested in heavy-meson-nucleus systems such as the $\eta'(958)$ meson for studies of $U_A(1)$ anomaly effects [10–12], the ϕ meson for $\bar{s}s$ components of the nucleon and Okubo-Zweig-Iizuka (OZI) rule at finite density [13], and D mesons for charm meson properties in the nucleus [14]. Thus, we would like to study the two-nucleon pick-up reactions theoretically as a possible method suited to form heavy-meson-nucleus bound systems.

One of the most serious problems in the formation reactions of heavy-meson-nucleus systems is the large momentum transfer, as mentioned above. It is known that the matching condition of momentum and angular momentum transfers plays an important role in determining the largely populated subcomponents and it is also known that the best choice for our purpose is the total angular momentum transfer $J = 0$ state formation in recoilless kinematics in many cases. In the one-nucleon pick-up reactions which we have mainly considered so far, recoilless kinematics cannot be satisfied for the formation of meson bound states of heavier meson than the nucleon because of the large mass. Thus, we consider two-nucleon pick-up reactions in this paper to investigate the possibility of extending our study to the heavier meson region using these reactions. Actually, there was an attempt to observe the η -mesic state in the two-nucleon pick-up ${}^{27}\text{Al}(p, {}^3\text{He})$ reaction at COSY-GEM [15].

II. EFFECTIVE NUMBER FORMALISM FOR THE QUASIDEUTERON IN THE NUCLEUS

We formulate the formation cross section of the heavy meson bound states by two-nucleon pick-up reactions. As we will see below, our model is so simple that it can be applied generally to heavy-meson bound-state formation by two-nucleon pick-up reactions such as (γ, d) and ($p, {}^3\text{He}$).

We apply the effective number approach, which has been used for studies of the meson-nucleus bound states [4], to evaluate the formation rate of the bound systems in two-nucleon pick-up reactions. In the effective number approach, the formation cross section for two-nucleon pick-up reactions can be written as

$$\frac{d^2\sigma}{dE d\Omega} = \left(\frac{d\sigma}{d\Omega}\right)^{\text{ele}} \sum_f \frac{\Gamma}{2\pi} \frac{1}{\Delta E^2 + \Gamma^2/4} N_{\text{eff}}, \quad (1)$$

where $(d\sigma/d\Omega)^{\text{ele}}$ is the elementary cross section of meson production, and Γ is the width of the meson bound states. All combinations of the final states, labeled f , are summed to

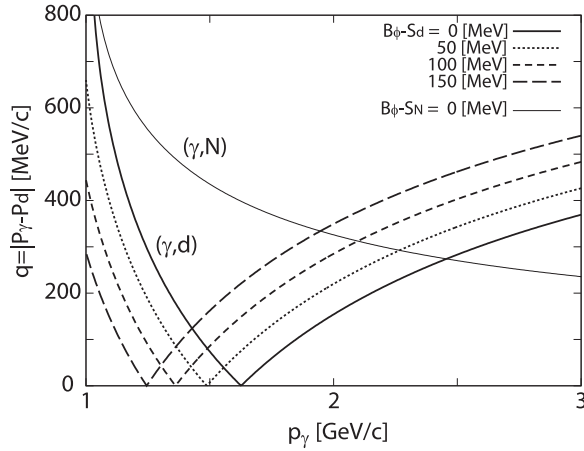


FIG. 1. Momentum transfer q of the forward (γ, d) reaction for the formation of $\phi(1020)$ meson bound states in the heavy target nucleus plotted as functions of the incident photon momentum p_γ for four values of the gap $(B_\phi - S_d)$ between the ϕ meson binding energy B_ϕ and the deuteron separation energy S_d as indicated in the figure. Momentum transfer of the one-nucleon pick-up (γ, N) reaction is also shown for comparison.

evaluate the inclusive cross section. The energy transfer ΔE of the reaction in the laboratory frame is defined as

$$\Delta E = (T_f + M_f) + (M - B) - (T_i + M_i) - (2M_N - S_{2N}), \quad (2)$$

where T_f and M_f are the kinetic energy and the mass of the emitted particle, T_i and M_i are the kinetic energy and the mass of the incident particle, and M is the mass of the produced meson. The meson binding energy B and the two-nucleon separation energy S_{2N} from the target nucleus are determined for each bound level of meson and excited level of the daughter nucleus. Here, we neglect the recoil energy of the nucleus.

The momentum transfer q of the reaction is defined as

$$\mathbf{q} = \mathbf{p}_i - \mathbf{p}_f \quad (3)$$

and is shown in Fig. 1 for the ϕ meson formation case, as an example, in the heavy target for the (γ, d) reaction together with that for the one-nucleon pick-up (γ, N) reaction as functions of the momentum of the incident photon. We also show the momentum transfers for the $(p, {}^3\text{He})$ and (p, d) reactions for ϕ meson formation in Fig. 2 for comparison. As we can see from the figures, the two-nucleon pick-up reactions satisfy the recoilless condition $q = 0$ at a finite incident momentum, while large momentum transfer is unavoidable for the one-nucleon pick-up reactions. We show in Fig. 3 the incident beam momenta p for the four reactions required to produce the meson with an effective mass M^* in recoilless kinematics. The effective mass M^* is defined as $M^* = M - B$ with meson mass M and binding energy B . We find clearly that the meson with a larger effective mass than the nucleon cannot be produced in recoilless kinematics by one-nucleon pick-up reactions. In two-nucleon pick-up reactions such as (γ, d) and $(p, {}^3\text{He})$, on the other hand, we can produce heavier meson states such as $\eta'(958)$, $\phi(1020)$, and $a_1(1260)$ meson bound states in recoilless kinematics.

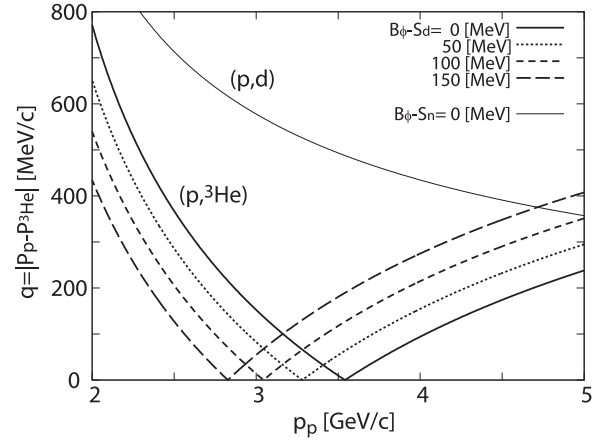


FIG. 2. Same as Fig. 1 except for the proton-induced $(p, {}^3\text{He})$ and (p, d) reactions.

The theoretical calculation of the two-nucleon pick-up reactions is in general rather difficult. In addition, we expect complicated nuclear excitations in daughter nuclei with two-nucleon holes, which will prevent us from clearly identifying meson bound states. Here, we consider as a target the specific nucleus ${}^6\text{Li}$, which has a well-developed cluster structure of $\alpha + d$ in the ground state. The probability of the $\alpha + d$ component included in the ground state of ${}^6\text{Li}$ is reported to be 0.616 in Ref. [16] and 0.73 in Ref. [17]. In the reaction considered in this paper, the momentum transfer to the initial deuteron wave function in ${}^6\text{Li}$ and the final meson wave function in the mesic nucleus is considered to be small near recoilless kinematics and the quasideuteron picture in the ${}^6\text{Li}$ target is expected to be a good approximation. Thus, by considering nuclei such as ${}^6\text{Li}$, which have a large quasideuteron component, as targets, we can evaluate the reaction rate in a simple way and expect to have the simple structure of the formation spectra of mesic nuclei in the two-nucleon pick-up reactions. In our model, we treat ${}^6\text{Li}$ as the bound state of the α particle and the deuteron

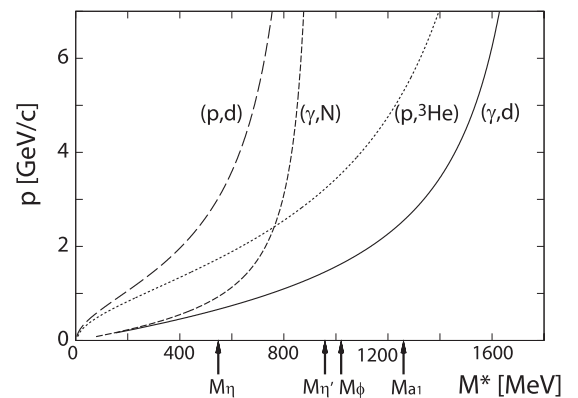


FIG. 3. Incident beam momenta p required to produce mesons in recoilless kinematics in one-nucleon pick-up $[(\gamma, N), (p, d)]$ and two-nucleon pick-up $[(\gamma, d), (p, {}^3\text{He})]$ reactions plotted as functions of meson effective mass M^* , which is defined as $M^* = M - B$ with meson mass M and binding energy B . The in-vacuum masses of η , η' , ϕ , and a_1 are indicated in the figure by arrows.

to evaluate the reaction rate. Thus, B in Eq. (2) is the binding energy of a heavy meson and α particle in the final state and S_{2N} is fixed to be $S_{2N} = 1.47$ MeV from the mass gap of initial and final nuclei as $S_{2N} = (M_\alpha + M_d) - M_{^6\text{Li}}$. The elementary cross section $(d\sigma/d\Omega)^{\text{el}}$ for meson production appearing in Eq. (1) is that of the $i + d \rightarrow f + \text{meson}$ reaction with incident particle i and emitted particle f , which should be evaluated from experiments as in previous cases [4–6]. Here, the emitted particle f will be ^3He for the proton-induced ($i = \text{proton}$) case and d for the γ -induced ($i = \text{photon}$) case, respectively.

In our model considering the ^6Li nucleus as the bound state of α particle and deuteron, the effective number N_{eff} of the $^6\text{Li}(i, f)\alpha \otimes \text{meson}$ reaction can be written as

$$N_{\text{eff}} = \sum_{JM} \left| \int \chi_f^*(\mathbf{r}) [\phi_m^*(\mathbf{r}) \otimes \psi_{1d}(\mathbf{r})]_{JM} \chi_i(\mathbf{r}) d\mathbf{r} \right|^2, \quad (4)$$

where $\phi_m(\mathbf{r})$ is the wave function of the meson bound state and $\psi_{1d}(\mathbf{r})$ that of the deuteron bound to the α in the ^6Li target. $\chi_i(\mathbf{r})$ and $\chi_f(\mathbf{r})$ are the incident and the emitted particle wave functions in the scattering states, respectively. We assume plane waves for χ_i and χ_f in this paper. The distortion effects of χ_i and χ_f depend on the incident and emitted particles [8]; however, they are known to be relatively small for the cases satisfying the matching condition [4]. The deuteron wave function ψ_{1d} in ^6Li is determined to reproduce the momentum distribution reported in Ref. [17] based on the analysis of the $^6\text{Li}(e, e'd)^4\text{He}$ reaction. We calculate ψ_{1d} by solving the Schrödinger equation with the Woods-Saxon-type potential,

$$U(r) = \frac{U_0}{1 + \exp[(r - R)/a]}, \quad (5)$$

and adjust the potential depth U_0 and the radius parameter R to reproduce the momentum distribution $\rho(p)$ reported in Ref. [17]. $\rho(p)$ is defined as

$$\rho(p) = \frac{1}{(2\pi)^3} \left| \int e^{-ip \cdot r} \psi_{1d}(\mathbf{r}) d\mathbf{r} \right|^2, \quad (6)$$

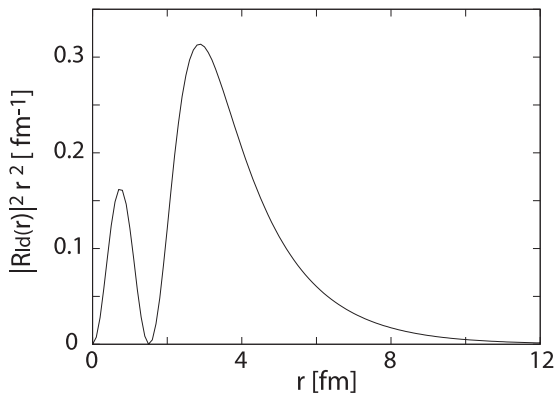


FIG. 4. Calculated density distribution of the radial part $R_{1d}(r)$ of the relative wave function $\psi_{1d}(\mathbf{r})$ of the α particle and the deuteron in the ^6Li nucleus.

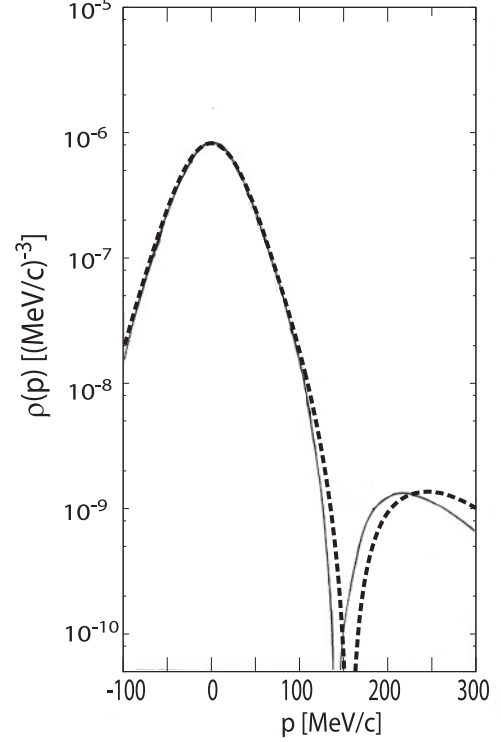


FIG. 5. Momentum distribution of the deuteron in ^6Li obtained by our model (dashed line) and by the analysis of the experimental data [17] (solid line). The results of our model are multiplied by the correction factor 0.73 to satisfy the same normalization as in Ref. [17].

where $|\psi_{1d}(\mathbf{r})|^2$ is normalized to be 1 in the coordinate space as usual. The potential parameters used here are fixed to be $R = 2.0$ fm, $a = 0.5$ fm, and $U_0 = -75$ MeV. The calculated wave function is shown in Fig 4 and the momentum distribution is shown in Fig. 5. The wave function in Fig. 4 corresponds to the $2s$ bound state as indicated in Ref. [17] because of the Pauli effect to nucleons, which forbids the α and deuteron clusters from being in the relative $1s$ state. The calculated momentum distribution reproduces the plane wave impulse approximation (PWIA) result in Ref. [17] reasonably well, as shown in the Fig. 5. In Fig. 5, we multiply our results by a factor 0.73 to correct the overall normalization of $\rho(p)$ to be the same as Ref. [17]. It should be noted that the PWIA results in Ref. [17] ignoring the distortion effects are the quantity which should be compared with our results calculated by Eq. (6).

The bound-meson wave functions $\phi_m(\mathbf{r})$ in the final state are calculated by solving the Klein-Gordon equation with the optical potential in the Woods-Saxon form as in Eq. (5). We fix the meson mass to be $M = 1020$ MeV as the ϕ meson, which is heavier than the nucleon and cannot be formed in recoilless kinematics in one-nucleon pick-up reactions. Since mesons can be absorbed by the nucleus generally, the potential strength U_0 in Eq. (5) is considered to be a complex number as $U_0 = (V_0 + iW_0)$ for mesons. In the present calculation, we consider a few potential strengths as examples and study how the two-nucleon pick-up reaction spectra change according to the meson-nucleus interaction. We consider first the potential strengths based on the data obtained by the

TABLE I. Calculated binding energies and widths of the meson- α bound states in units of MeV with the potential strength $(V_0, W_0) =$ (i) $(-34.7, -7.5)$, (ii) $(-250, -5)$, and (iii) $(-250, -20)$ MeV. The meson mass is fixed to be 1020 MeV.

(n_ϕ, ℓ_ϕ) state	(i)		(ii)		(iii)	
	B.E.	Γ	B.E.	Γ	B.E.	Γ
1s	0.76	2.9	131.5	8.1	131.2	32.5
2s			14.5	2.8	14.2	11.2
2p			58.0	5.5	57.7	21.8
3d			2.9	2.8	2.4	11.3

E325 experiment in KEK (High Energy Accelerator Research Organization) [18], where the ϕ meson mass shift is reported as $\Delta m(\rho_0)/m = -3.4\%$ and the ϕ meson width in the nucleus is $\Gamma_\phi(\rho_0) = 15$ MeV. We adopt these numbers as the ϕ mesic optical potential and fix this as $(V_0, W_0) = (-34.7, -7.5)$ MeV. We mention here that the large in-medium width $\Gamma_\phi(\rho_0) \simeq 80$ MeV of the ϕ meson was also indicated based on another attenuation experiment by Laser Electron Photon beamline at SPring-8 [19], which corresponds to an imaginary potential strength $W_0 = -40$ MeV. We have checked numerically that the potential with this imaginary strength together with the real-part strength corresponding to the 3.4% mass reduction does not provide ϕ meson bound states in the α potential. We then assume a stronger attractive potential for the meson-nucleus system to estimate the formation rate of heavy-meson bound systems with a strong attractive potential as reported in Ref. [11] for the $\eta'(958)$ meson in a theoretical model. The assumed potential parameters with two different absorption strengths: $(V_0, W_0) = (-250, -5)$ and $(-250, -20)$ in units of MeV. The distribution parameters are fixed to be $R = 1.18A^{1/3} - 0.48$ fm and $a = 0.5$ fm with $A = 4$ for the meson- α system. We show in Table I the calculated binding energies and widths of the meson bound states for the three different potentials. The radial density distributions are also shown in Fig. 6 for $(V_0, W_0) = (-34.7, -7.5)$ and $(-250, -5)$ MeV cases. We found that the radial density distributions of 1s states of the two potentials are very different because of the different potential strength.

Since the angular momentum l_d of the relative wave function of the deuteron and the α particle in ${}^6\text{Li}$ is considered to be 0, the expression for the effective numbers in Eq. (4) can be simplified as

$$N_{\text{eff}} = \sum_M \left| \int e^{iq \cdot r} \phi_{l_m}^*(\mathbf{r}) \psi_0(\mathbf{r}) d\mathbf{r} \right|^2, \quad (7)$$

in the plane-wave approximation. We use this expression to calculate the effective numbers in this paper.

In recoilless kinematics, only s states of the meson bound states can be populated because of the orthogonality of the angular part of the wave function, as can be seen in Eq. (7). And because of the approximate orthogonality of the radial parts of ϕ_{l_m} and ψ_0 , the substitutional $2s$ state of the meson is expected to be largely populated.

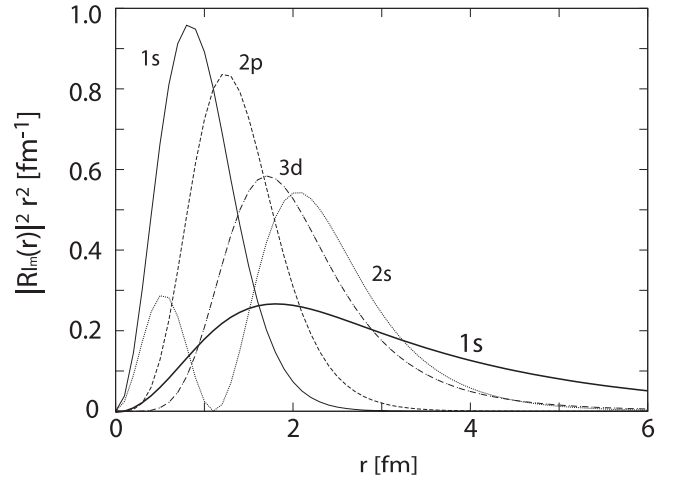


FIG. 6. Calculated density distribution of the radial part $R_{l_m}(r)$ of the wave function $\phi_{l_m}(\mathbf{r})$ of the meson bound state in the α particle for the potential strength $(V_0, W_0) = (-34.7, -7.5)$ MeV (thick solid line) and $(-250, -5)$ MeV (thin lines).

III. NUMERICAL RESULT FOR BOUND-STATE FORMATION RATE

To investigate the momentum transfer dependence of N_{eff} for each bound-state formation, we show in Fig. 7 the calculated effective numbers N_{eff} by Eq. (7) as functions of the momentum transfer $|\mathbf{q}|$ for two-nucleon pick-up reactions for a ${}^6\text{Li}$ target. Each effective number has a characteristic behavior due to the matching condition of the momentum transfer and the angular momentum transfer. As we have mentioned in the previous section, the effective numbers N_{eff} are exactly 0 for $2p$ and $3d$ states at $|\mathbf{q}| = 0$ because of the orthogonality condition of the angular part wave function to the s -wave function ψ_0 . And the substitutional $2s$ state of the

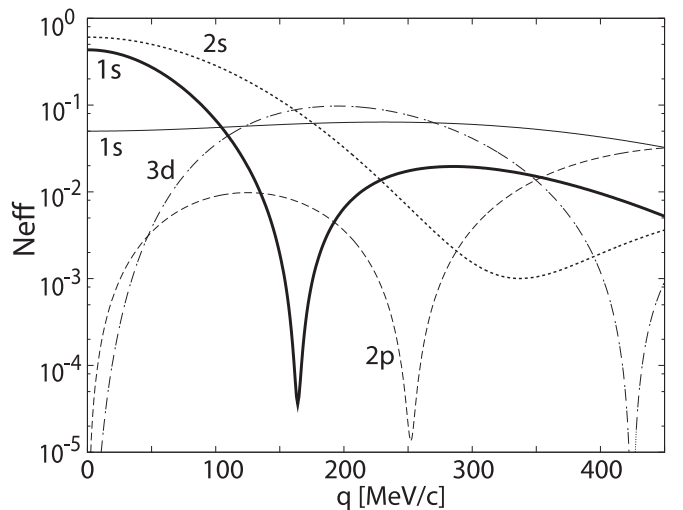


FIG. 7. Calculated effective numbers plotted as functions of the momentum transfer of the two-nucleon pick-up reactions for ${}^6\text{Li}$ target for the 1s meson-bound-state formation with the potential strength $(V_0, W_0) = (-34.7, -7.5)$ MeV (thick solid line) and the 1s, 2s, 2p, and 3d bound states with $(V_0, W_0) = (-250, -5)$ MeV (thin lines).

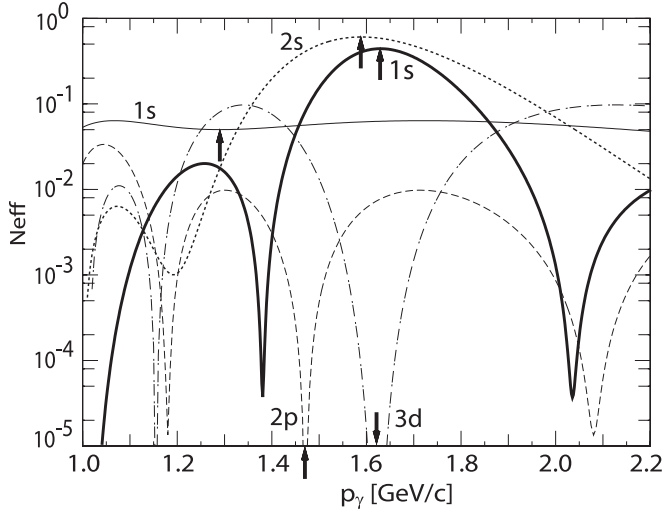


FIG. 8. Same as Fig. 7 except for the plots as functions of the incident photon momentum p_γ for the (γ, d) reaction. The arrow indicates the incident photon momentum of the recoilless kinematics for each meson-bound-state formation.

bound meson has the largest contribution at $|q| = 0$ as we expected. The contribution of the $1s$ state with weaker real potential $V_0 = -34.7$ MeV has the stronger dependence on q , as naturally expected because of its larger special dimensions, as shown in Fig. 6. As the momentum transfer increases, the $3d$ bound-state formation has the largest contribution at $160 \lesssim |q| \lesssim 270$ MeV/c and then the $1s$ bound state at $270 \lesssim |q| \lesssim 450$ MeV/c. The overall strength of the heavy-meson bound-state formation cross section becomes smaller for kinematics with larger momentum transfer.

We show the same effective numbers as functions of the incident particle energies for (γ, d) and $(p, {}^3\text{He})$ reactions in Figs. 8 and 9. Because of the different binding energies of the meson appearing in Eq. (2), the incident particle energy which

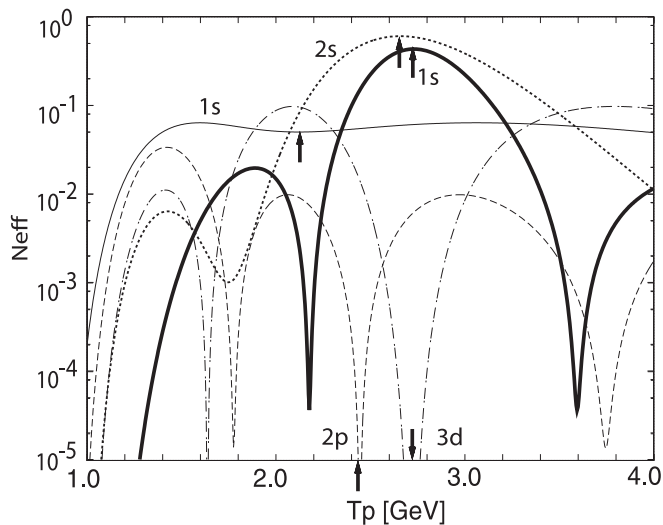


FIG. 9. Same as Fig. 7 except for the plots as functions of the incident proton kinetic energy T_p for the $(p, {}^3\text{He})$ reaction. The arrow indicates the incident proton kinetic energy of the recoilless kinematics for each meson-bound-state formation.

corresponds to recoilless kinematics ($|q| = 0$) is different for each bound state. We indicate the incident particle energy of the recoilless kinematics for each state by the arrow in Figs. 8 and 9. The figures show very similar behavior for N_{eff} .

We find that the substitutional $2s$ state of the meson is produced in the almost recoilless condition and has the largest contribution to the cross section at $p_\gamma = 1.6$ GeV/c ($T_p = 2.7$ GeV). [In the explanation below, we indicate the photon momentum p_γ in the (γ, d) reaction with the corresponding proton kinetic energy T_p in the $(p, {}^3\text{He})$ reaction in parentheses.] We mention here that the $1s$ state wave function with potential strength $(V_0, W_0) = (-34.7, -7.5)$ MeV has a larger spatial dimension, which violates the approximate orthogonality of the radial part with ψ_0 at $q = 0$ in Eq. (7), and thus the contribution of this $1s$ state also has a large contribution at $p_\gamma = 1.6$ GeV/c ($T_p = 2.7$ GeV). At $p_\gamma = 1.35$ GeV/c ($T_p = 2.1$ GeV), a little above the ϕ production threshold of the elementary process, the sizes of the effective numbers of the $2s$ and $3d$ states are similar and larger than those of other state formations. At $p_\gamma = 1.8$ GeV/c ($T_p = 3.1$ GeV), the effective number of the $2s$ state formation is still dominant; however, the other contributions of the $1s$ and $3d$ state formations become relatively more important than at $p_\gamma = 1.6$ GeV/c ($T_p = 2.7$ GeV). The contributions of the $1s$, $2s$, and $3d$ state formations are important at $p_\gamma = 2.0$ GeV/c ($T_p = 3.5$ GeV) and the formation spectrum is expected to be a little more complicated than those at other photon momenta. We find that N_{eff} for the $2s$ bound-state formation takes the largest value $N_{\text{eff}} = 0.606$ at $p_\gamma = 1.59$ GeV/c ($T_p = 2.66$ GeV), which means that the meson-bound-state formation cross section can be about half of the elementary cross section.

We then calculate the relative strength of the formation spectra of the meson bound states in the α particle by the two-nucleon pick-up reaction in a ${}^6\text{Li}$ target at incident photon momenta $p_\gamma = 1.35, 1.6, 1.8,$ and 2.0 GeV/c for the (γ, d) reaction, which corresponds to $T_p = 2.1, 2.7, 3.1,$ and 3.5 GeV for the $(p, {}^3\text{He})$ reaction. We can expect to observe different behavior of the formation spectra at these energies as expected from the energy dependence of the effective numbers. The calculated $\frac{d^2\sigma}{dE d\Omega} / (\frac{d\sigma}{d\Omega})^{\text{ele}}$ results for the (γ, d) reaction are shown in Fig. 10 for three different optical potential parameters for the meson bound in the α particle.

The expected spectra for the potential strength $(V_0, W_0) = (-34.7, -7.5)$ MeV case are simple since there is only a lightly bound $1s$ state. As shown in Figs. 10(b) and 10(c), this $1s$ state is seen as a peak close to this meson production threshold for $p_\gamma = 1.6$ and 1.8 GeV/c ($T_p = 2.7$ and 3.1 GeV). The contribution of this state has such a strong q and incident energy dependence, as shown in Figs. 7–9, that it becomes smaller than those with deeper potential cases and invisible in Figs. 10(a) and 10(d).

For deeper potential cases with $(V_0, W_0) = (-250, -5)$ and $(-250, -20)$ MeV, we find that the spectra at $p_\gamma = 1.6$ and 1.8 GeV/c ($T_p = 2.7$ and 3.1 GeV) are dominated by the $2s$ state formation and the other contributions are significantly smaller. On the other hand, we can observe clear peak structures of the $1s$ and $3d$ state formations in addition

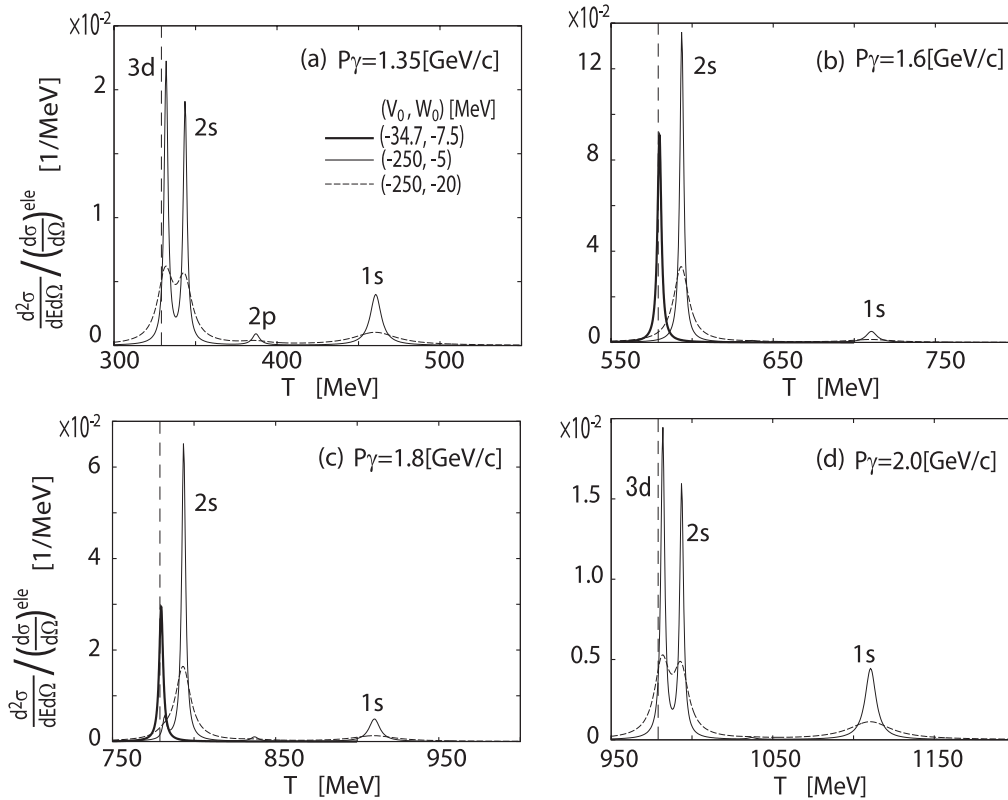


FIG. 10. Expected spectra of the forward two-nucleon pick-up (γ, d) reaction ${}^6\text{Li}$ for the formation of the meson- α bound states plotted as functions of the emitted deuteron kinetic energy for the incident photon momenta $p_\gamma =$ (a) 1.35, (b) 1.6, (c) 1.8, and (d) 2.0 GeV/c. The vertical dashed line indicates the meson production threshold. Each line is calculated with different optical potential parameters for the meson- α system as indicated in (a). The spectrum with the potential $(V_0, W_0) = (-34.7, 7.5)$ MeV is only shown in (b) and (c) because it is small and invisible in (a) and (d).

to the $2s$ state at $p_\gamma = 1.35$ and 2.0 GeV/c ($T_p = 2.1$ and 3.5 GeV). The spectra $\frac{d^2\sigma}{dE d\Omega} / (\frac{d\sigma}{d\Omega})^{ele}$ values are relatively large at $p_\gamma = 1.6$ and 1.8 GeV/c ($T_p = 2.7$ and 3.1 GeV) where the momentum transfer of the two-nucleon pick-up reactions is small. At $p_\gamma = 1.8$ and 2.0 GeV/c ($T_p = 3.1$ and 3.5 GeV), the momentum transfer is larger and the size of the spectra becomes smaller rapidly for the larger incident momentum and energy. We also show the effects of the imaginary part of the optical potential on the formation spectra in Fig. 10. Since we have only one deuteron state in the initial nucleus ${}^6\text{Li}$, the reaction spectra have a simple structure, especially for $(V_0, W_0) = (-34.7, -7.5)$ MeV. Thus, the main effects of the absorptive potential are found to reduce the height of the peak with large width. The overlap of the resonance peaks due to the widths only occurs between $2s$ and $3d$ states for the absorption potential strengths studied here in the two-nucleon pick-up spectra.

If the imaginary potential is large (e.g., $W_0 = -40$ MeV), as indicated based on the data reported for the ϕ meson in Ref. [19], the height of all peaks in the spectra shown in Fig. 10 becomes lower in inverse proportion to the strength of the imaginary potential, and the contributions of $2s$ and $3d$ states for the $V_0 = -250$ MeV case cannot be distinguished because of the large widths.

IV. SUMMARY

We have considered two-nucleon pick-up reactions to investigate the feasibility of the reactions of this type to extend our research field of meson-nucleus bound systems to the heavier meson region. We have developed a model and used the effective number approach to evaluate the formation rate. As an example, we have applied the model to the heavy-meson bound-state formation in an α particle with a ${}^6\text{Li}$ target. As shown in the numerical results, we have found that the shape of the formation spectra is simple and seems to be suited to extract the binding energies and widths of the meson bound state because of the simple α - d cluster structure of ${}^6\text{Li}$. The size of the formation cross section can be more than half of the elementary cross section at recoilless kinematics.

This theoretical model is so simple that we can apply it easily to evaluate the mesic nucleus formation rate of other two-nucleon pick-up reactions such as (π, d) . To do this, we simply replace the elementary cross sections with those of the appropriate processes of meson production such as $\pi + d \rightarrow d + \text{heavy meson}$. In this model, however, the target nucleus is required to have a large component of the quasideuteron structure. Thus, we have considered the ${}^6\text{Li}$ target as an example in this paper. The calculated spectral shapes are expected to have simple structure generally because of the existence

of the quasideuteron in the target nucleus and are suited for extracting meson properties from the reaction spectra.

In general cases, we should not assume the existence of the quasideuteron in the target nuclei [20] and we need to evaluate the emissions of a deuteron composed of two nucleons which are in different single-particle levels in the target. The deuteron can be formed from any pair of protons and neutrons in the target by the reaction of meson production. In this process, however, the spectral shape could be so complicated that it is difficult to extract meson properties.

With actual experimental observations, the calculated cross sections could be too small to find peak structures in the inclusive missing mass spectra due to the size of the elementary cross section, and coincidence measurements to detect the particle pair emissions from meson absorption in the nucleus may be necessary to reduce the background. So far, the formation of an η mesic nucleus in the two-nucleon pick-up ($p, {}^3\text{He}$) reaction for an ${}^{27}\text{Al}$ target was reported by Budzanowski *et al.* (COSY-GEM). They performed the coincidence measurement with $p\pi^-$ pair emissions from ηN in the nucleus. They reported 0.5 nb for the upper limit of the signal of the η mesic nuclear formation cross section [15] at an energy where the elementary cross section is 77 nb/sr [21]. In our example

considered here, the effective number N_{eff} for the formation of the meson bound state is about 0.5 for both shallow and deep potential cases around $p_\gamma = 1.6$ GeV/ c ($T_p = 2.7$ GeV) for the largest contributions, as shown in Fig. 8. In this sense, we think the present result also has relevance as a guide for the actual experiment.

We believe that it is quite important to find new reactions suited for forming heavy-meson bound states in the nucleus to explore the various aspects of the strong interaction symmetries at finite density by the mesic nuclei. In this context, the two-nucleon pick-up reactions studied in this paper are quite interesting, since we can satisfy the recoilless condition in this reaction for the formation of a meson heavier than the nucleon.

ACKNOWLEDGMENTS

We acknowledge fruitful discussions with H. Fujioka and K. Itahashi. N.I. appreciates the support by the Grant-in-Aid for Scientific Research by the JSPS (No. 23-2274). This work was partly supported by the Grants-in-Aid for Scientific Research (No. 22740161, No. 20540273, and No. 22105510). This work was done in part under the Yukawa International Program for Quark-hadron Sciences (YIPQS).

-
- [1] T. Hatsuda and T. Kunihiro, *Phys. Rep.* **247**, 221 (1994), and references therein.
- [2] D. Jido, T. Hatsuda, and T. Kunihiro, *Phys. Lett. B* **670**, 109 (2008).
- [3] E. E. Kolomeitsev, N. Kaiser, and W. Weise, *Phys. Rev. Lett.* **90**, 092501 (2003).
- [4] H. Toki, S. Hirenzaki, T. Yamazaki and R. S. Hayano, *Nucl. Phys. A* **501**, 653 (1989); S. Hirenzaki, H. Toki, and T. Yamazaki, *Phys. Rev. C* **44**, 2472 (1991); H. Toki, S. Hirenzaki, and T. Yamazaki, *Nucl. Phys. A* **530**, 679 (1991).
- [5] T. Kishimoto, *Phys. Rev. Lett.* **83**, 4701 (1999); S. Hirenzaki, Y. Okumura, H. Toki, E. Oset, and A. Ramos, *Phys. Rev. C* **61**, 055205 (2000); K. Ikuta, M. Arima, and K. Masutani, *Prog. Theor. Phys.* **108**, 917 (2002); J. Yamagata, H. Nagahiro, Y. Okumura, and S. Hirenzaki, *ibid.* **114**, 301 (2005); **114**, 905(E) (2005); J. Yamagata, H. Nagahiro, and S. Hirenzaki, *Phys. Rev. C* **74**, 014604 (2006).
- [6] Q. Haider and L. C. Liu, *Phys. Lett. B* **172**, 257 (1986); R. S. Hayano, S. Hirenzaki, and A. Gillitzer, *Eur. Phys. J. A* **6**, 99 (1999); D. Jido, H. Nagahiro, and S. Hirenzaki, *Phys. Rev. C* **66**, 045202 (2002); H. Nagahiro, D. Jido, and S. Hirenzaki, *ibid.* **68**, 035205 (2003); D. Jido, E. E. Kolomeitsev, H. Nagahiro, and S. Hirenzaki, *Nucl. Phys. A* **811**, 158 (2008).
- [7] K. Suzuki *et al.*, *Phys. Rev. Lett.* **92**, 072302 (2004).
- [8] H. Nagahiro, D. Jido, and S. Hirenzaki, *Nucl. Phys. A* **761**, 92 (2005).
- [9] H. Nagahiro, D. Jido, and S. Hirenzaki, *Phys. Rev. C* **80**, 025205 (2009).
- [10] H. Nagahiro and S. Hirenzaki, *Phys. Rev. Lett.* **94**, 232503 (2005).
- [11] H. Nagahiro, M. Takizawa, and S. Hirenzaki, *Phys. Rev. C* **74**, 045203 (2006).
- [12] D. Jido, H. Nagahiro, and S. Hirenzaki, arXiv:1109.0394 [nucl-th].
- [13] J. Yamagata-Sekihara, S. Hirenzaki, D. Cabrera, and M. J. Vicente-Vacas, *Prog. Theor. Phys.* **124**, 147 (2010).
- [14] C. Garca-Recio, J. Nieves, and L. Tolos, *Phys. Lett. B* **690**, 369 (2010).
- [15] A. Budzanowski *et al.*, *Phys. Rev. C* **79**, 012201(R) (2009).
- [16] W. C. Parke and D. R. Lehman, *Phys. Rev. C* **29**, 2319 (1984).
- [17] R. Ent *et al.*, *Phys. Rev. Lett.* **57**, 2367 (1986).
- [18] R. Muto *et al.* (KEK-PS. E325 Collaboration), *Phys. Rev. Lett.* **98**, 042501 (2007).
- [19] T. Ishikawa *et al.*, *Phys. Lett. B* **608**, 215 (2005).
- [20] E. C. Simpson and J. A. Tostevin, *Phys. Rev. C* **83**, 014605 (2011).
- [21] P. Berthet *et al.*, *Nucl. Phys. A* **443**, 589 (1985).